Inclusive Jet Production in $p\bar{p}$ Collisions

B. Abbott,[56] A. Abdesselam,[11] M. Abolins,[49] V. Abramov,[24] B. S. Acharya,[16] D. L. Adams,[58] M. Adams,[36] G. A. Alves,[2] N. Amos,[2] E. W. Anderson,[41] M. M. Baarmand,[53] V. V. Babintsev,[24] L. Babukhadia,[53] T. C. Bacon,[26] A. Baden,[45] B. Baldin,[35] P. W. Balm,[19] S. Banerjee,[16] E. Barberis,[28] P. Baringer,[42] J. F. Bartlett,[35] U. Bassler,[12] D. Bauer,[26] A. Bean,[42] M. Begel,[52] A. Belyaev,[23] S. B. Beri,[14] G. Bernardi,[12] I. Bertram,[25] A. Besson,[9] R. Beuselinck,[26] V. A. Bezzubov,[24] P. C. Bhat,[35] V. Bhatnagar,[11] M. Bhattacharjee,[53] G. Blazey,[37] S. Blessing,[33] A. Boehnlein,[35] N. I. Bojko,[24] F. Borcherding,[35] A. Brandt,[58] R. Breedon,[29] G. Briskin,[57] R. Brock,[49] G. Brooijmans,[35] A. Bross,[35] D. Buchholz,[38] M. Buehler,[36] V. Buescher,[52] V. S. Burtovoi,[24] J. M. Butler,[46] F. Canelli,[52] W. Carvalho,[3] D. Casey,[49] Z. Casilum,[53] H. Castilla-Valdez,[18] D. Chakraborty,[53] K. M. Chan,[52] S. V. Chekulaev,[24] D. K. Cho,[52] S. Choi,[32] S. Chopra,[54] J. H. Christenson,[35] M. Chung,[36] D. Claes,[50] A. R. Clark,[28] J. Cochran,[32] L. Coney,[40] B. Connolly,[33] W. E. Cooper,[35] D. Coppage,[42] M. A. C. Cummings,[37] D. Cutts,[57] G. A. Davis,[52] K. Davis,[27] K. De,[58] K. Del Signore,[48] M. Demarteau,[35] R. Demina,[43] P. Demine,[9] D. Denisov,[35] S. P. Denisov,[24] S. Desai,[53] H. T. Diehl,[35] M. Diesburg,[35] G. Di Loreto,[49] S. Doulas,[47] P. Draper,[58] Y. Ducros,[13] L. V. Dudko,[23] S. Duensing,[20] L. Duflot,[11] S. R. Dugad,[16] A. Dyshkant,[24] D. Edmunds,[49] J. Ellison,[32] V. D. Elvira,[35] R. Engelmann,[53] S. Eno,[45] G. Eppley,[60] P. Ermolov,[23] O. V. Eroshin,[24] J. Estrada,[52] H. Evans,[51] V. N. Evdokimov,[24] T. Fahland,[31] S. Feher,[35] D. Fein,[27] T. Ferbel,[52] H. E. Fisk,[35] Y. Fisyak,[54] E. Flattum,[35] F. Fleuret,[28] M. Fortner,[37] K. C. Frame,[49] S. Fuess,[35] E. Gallas,[35] A. N. Galyaev,[24] M. Gao,[51] V. Gavrilov,[22] R. J. Genik II,[25] K. Genser,[35] C. E. Gerber,[36] Y. Gershtein,[57] R. Gilmartin,[33] G. Ginther,[52] B. Gómez,[5] G. Gómez,[45] P. I. Goncharov,[24] J. L. González Solís,[18] H. Gordon,[54] L. T. Goss,[59] K. Gounder,[32] A. Goussiou,[53] N. Graf,[54] G. Graham,[45] P. D. Grannis,[53] J. A. Green,[41] H. Greenlee,[35] S. Grinstein,[1] L. Groer,[51] S. Grünendahl,[35] A. Gupta,[16] S. N. Gurzhiev,[24] G. Gutierrez,[35] P. Gutierrez,[56] N. J. Hadley,[45] H. Haggerty,[35] S. Hagopian,[33] V. Hagopian,[33] K. S. Hahn,[52] R. E. Hall,[30] P. Hanlet,[47] S. Hansen,[35] J. M. Hauptman,[41] C. Hays,[51] C. Hebert,[42] D. Hedin,[37] A. P. Heinson,[32] U. Heintz,[46] T. Heuring,[33] R. Hirosky,[61] J. D. Hobbs,[53] B. Hoeneisen,[8] J. S. Hoftun,[57] S. Hou,[48] Y. Huang,[48] R. Illingworth,[26] A. S. Ito,[35] M. Jaffré,[11] S. A. Jerger,[1] R. Jesik,[39] K. Johns,[27] M. Johnson,[35] A. Jonckheere,[35] M. Jones,[34] H. Jöstlein,[35] A. Juste,[35] S. Kahn,[54] E. Kajfasz,[10] D. Karmanov,[23] D. Karmgard,[40] S. K. Kim,[17] B. Klima,[35] C. Klopfenstein,[29] B. Knuteson,[28] W. Ko,[29] J. M. Kohli,[14] A. V. Kostritskiy,[24] J. Kotcher,[54] A. V. Kotwal,[51] A. V. Kozelov,[24] E. A. Kozlovsky,[24] J. Krane,[41] M. R. Krishnaswamy,[16] S. Krzywdzinski,[35] M. Kubantsev,[43] S. Kuleshov,[22] Y. Kulik,[53] S. Kunori,[45] V. E. Kuznetsov,[32] G. Landsberg,[57] A. Leflat,[23] C. Leggett,[28] F. Lehner,[35] J. Li,[58] Q. Z. Li,[35] J. G. R. Lima,[3] D. Lincoln,[35] S. L. Linn,[33] J. Linnemann,[49] R. Lipton,[35] A. Lucotte,[9] L. Lueking,[35] C. Lundstedt,[50] C. Luo,[39] A. K. A. Maciel,[37] R. J. Madaras,[28] V. Manankov,[23] H. S. Mao,[4] T. Marshall,[39] M. I. Martin,[35] R. D. Martin,[36] K. M. Mauritz,[41] B. May,[38] A. A. Mayorov,[39] R. McCarthy,[53] J. McDonald,[33] T. McMahon,[55] H. L. Melanson,[35] X. C. Meng,[4] M. Merkin,[23] K. W. Merritt,[35] C. Miao,[57] H. Miettinen,[60] D. Mihalcea,[56] C. S. Mishra,[35] N. Mokhov,[35] N. K. Mondal,[16] H. E. Montgomery,[35] R. W. Moore,[49] M. Mostafa,[1] H. da Motta,[2] E. Nagy,[10] F. Nang,[27] M. Narain,[46] V. S. Narasimham,[16] H. A. Neal,[48] J. P. Negret,[5] S. Negroni,[10] D. Norman,[59] T. Nunnemann,[35] L. Oesch,[48] V. Oguri,[3] B. Olivier,[12] N. Oshima,[35] P. Padley,[60] L. J. Pan,[38] K. Papageorgiou,[26] A. Para,[35] N. Parashar,[47] R. Partridge,[57] N. Parua,[53] M. Paterno,[52] A. Patwa,[53] B. Pawlik,[21] J. Perkins,[58] M. Peters,[34] O. Peters,[19] P. Pétroff,[11] R. Piegaia,[1] H. Piekarz,[33] B. G. Pope,[49] E. Popkov,[46] H. B. Prosper,[33] S. Protopopescu,[54] J. Qian,[48] P. Z. Quintas,[35] R. Raja,[35] S. Rajagopalan,[54] E. Ramberg,[35] P. A. Rapidis,[35] N. W. Reay,[43] S. Reucroft,[47] J. Rha,[32] M. Ridel,[11] M. Rijssenbeek,[53] T. Rockwell,[49] M. Roco,[35] P. Rubinov,[35] R. Ruchti,[40] J. Rutherfoord,[27] A. Santoro,[2] L. Sawyer,[44] R. D. Schamberger,[53] H. Schellman,[38] A. Schwartzman,[1] N. Sen,[60] E. Shabalina,[23] R. K. Shivpuri,[15] D. Shpakov,[47] M. Shupe,[27] R. A. Sidwell,[43] V. Simak,[7] H. Singh,[32] J. B. Singh,[14] V. Sirotenko,[35] P. Slattery,[52] E. Smith,[56] R. P. Smith,[35] R. Snihur,[38] G. R. Snow,[50] J. Snow,[55] S. Snyder,[54] J. Solomon,[36] V. Sorín,[1] M. Sosebee,[58] N. Sotnikova,[23] K. Soustruznik,[6] M. Souza,[2] N. R. Stanton,[43] G. Steinbrück,[51] R. W. Stephens,[58] F. Stichelbaut,[54] D. Stoker,[31] V. Stolin,[22] D. A. Stoyanova,[24] M. Strauss,[56] M. Strovink,[28] L. Stutte,[35] A. Sznajder,[3] W. Taylor,[53] S. Tentindo-Repond,[33] J. Thompson,[45] D. Toback,[45] S. M. Tripathi,[29] T. G. Trippe,[28] A. S. Turcot,[54] P. M. Tuts,[51] P. van Gemmeren,[35] V. Vaniev,[24] R. Van Kooten,[39] N. Varelas,[36] A. A. Volkov,[24] A. P. Vorobiev,[24] H. D. Wahl,[33] H. Wang,[38] Z.-M. Wang,[53] J. Warchol,[40] G. Watts,[62] M. Wayne,[40] H. Weerts,[49] A. White,[58] J. T. White,[59] D. Whiteson,[28] J. A. Wightman,[41] D. A. Wijngaarden,[20] S. Willis,[37] S. J. Wimpenny,[32] J. V. D. Wirjawan,[59] J. Womersley,[35] D. R. Wood,[47] R. Yamada,[35] P. Yamin,[54] T. Yasuda,[35] K. Yip,[54] S. Youssef,[33] J. Yu,[35] Z. Yu,[38] M. Zanabria,[5] H. Zheng,[40] Z. Zhou,[41] M. Zielinski,[52] D. Zieminska,[39] A. Zieminski,[39] V. Zutshi,[52] E. G. Zverev,[23] and A. Zylberstejn[13]

(D0 Collaboration)

[1]*Universidad de Buenos Aires, Buenos Aires, Argentina*
[2]*LAFEX, Centro Brasileiro de Pesquisas Físicas, Rio de Janeiro, Brazil*
[3]*Universidade do Estado do Rio de Janeiro, Rio de Janeiro, Brazil*
[4]*Institute of High Energy Physics, Beijing, People's Republic of China*
[5]*Universidad de los Andes, Bogotá, Colombia*
[6]*Charles University, Prague, Czech Republic*
[7]*Institute of Physics, Academy of Sciences, Prague, Czech Republic*
[8]*Universidad San Francisco de Quito, Quito, Ecuador*
[9]*Institut des Sciences Nucléaires, IN2P3-CNRS, Universite de Grenoble 1, Grenoble, France*
[10]*CPPM, IN2P3-CNRS, Université de la Méditerranée, Marseille, France*
[11]*Laboratoire de l'Accélérateur Linéaire, IN2P3-CNRS, Orsay, France*
[12]*LPNHE, Universités Paris VI and VII, IN2P3-CNRS, Paris, France*
[13]*DAPNIA/Service de Physique des Particules, CEA, Saclay, France*
[14]*Panjab University, Chandigarh, India*
[15]*Delhi University, Delhi, India*
[16]*Tata Institute of Fundamental Research, Mumbai, India*
[17]*Seoul National University, Seoul, Korea*
[18]*CINVESTAV, Mexico City, Mexico*
[19]*FOM-Institute NIKHEF and University of Amsterdam/NIKHEF, Amsterdam, The Netherlands*
[20]*University of Nijmegen/NIKHEF, Nijmegen, The Netherlands*
[21]*Institute of Nuclear Physics, Kraków, Poland*
[22]*Institute for Theoretical and Experimental Physics, Moscow, Russia*
[23]*Moscow State University, Moscow, Russia*
[24]*Institute for High Energy Physics, Protvino, Russia*
[25]*Lancaster University, Lancaster, United Kingdom*
[26]*Imperial College, London, United Kingdom*
[27]*University of Arizona, Tucson, Arizona 85721*
[28]*Lawrence Berkeley National Laboratory and University of California, Berkeley, California 94720*
[29]*University of California, Davis, California 95616*
[30]*California State University, Fresno, California 93740*
[31]*University of California, Irvine, California 92697*
[32]*University of California, Riverside, California 92521*
[33]*Florida State University, Tallahassee, Florida 32306*
[34]*University of Hawaii, Honolulu, Hawaii 96822*
[35]*Fermi National Accelerator Laboratory, Batavia, Illinois 60510*
[36]*University of Illinois at Chicago, Chicago, Illinois 60607*
[37]*Northern Illinois University, DeKalb, Illinois 60115*
[38]*Northwestern University, Evanston, Illinois 60208*
[39]*Indiana University, Bloomington, Indiana 47405*
[40]*University of Notre Dame, Notre Dame, Indiana 46556*
[41]*Iowa State University, Ames, Iowa 50011*
[42]*University of Kansas, Lawrence, Kansas 66045*
[43]*Kansas State University, Manhattan, Kansas 66506*
[44]*Louisiana Tech University, Ruston, Louisiana 71272*
[45]*University of Maryland, College Park, Maryland 20742*
[46]*Boston University, Boston, Massachusetts 02215*
[47]*Northeastern University, Boston, Massachusetts 02115*
[48]*University of Michigan, Ann Arbor, Michigan 48109*
[49]*Michigan State University, East Lansing, Michigan 48824*
[50]*University of Nebraska, Lincoln, Nebraska 68588*
[51]*Columbia University, New York, New York 10027*
[52]*University of Rochester, Rochester, New York 14627*
[53]*State University of New York, Stony Brook, New York 11794*
[54]*Brookhaven National Laboratory, Upton, New York 11973*
[55]*Langston University, Langston, Oklahoma 73050*
[56]*University of Oklahoma, Norman, Oklahoma 73019*
[57]*Brown University, Providence, Rhode Island 02912*
[58]*University of Texas, Arlington, Texas 76019*
[59]*Texas A&M University, College Station, Texas 77843*

^{60}*Rice University, Houston, Texas 77005*
^{61}*University of Virginia, Charlottesville, Virginia 22901*
^{62}*University of Washington, Seattle, Washington 98195*

We report a new measurement of the pseudorapidity (η) and transverse-energy (E_T) dependence of the inclusive jet production cross section in $p\bar{p}$ collisions at $\sqrt{s} = 1.8$ TeV using 95 pb^{-1} of data collected with the D0 detector at the Fermilab Tevatron. The differential cross section $d^2\sigma/(dE_T d\eta)$ is presented up to $|\eta| = 3$, significantly extending previous measurements. The results are in good overall agreement with next-to-leading order predictions from QCD and indicate a preference for certain parton distribution functions.

This past decade has witnessed impressive progress in both the theoretical and experimental understanding of the collimated streams of particles or "jets" that emerge from inelastic hadron collisions. Theoretically, jet production in hadron collisions is understood within the framework of quantum chromodynamics (QCD), as a hard scattering of the constituent partons (quarks and gluons) that, having undergone a collision, manifest themselves as jets in the final state. QCD predicts the amplitudes for the hard scattering of partons at high energies. Perturbative QCD calculations of jet cross sections [1–3], using accurately determined parton distribution functions (PDFs) [4,5], have increased the interest in jet measurements at the $\sqrt{s} = 1.8$ TeV Tevatron proton-antiproton collider. Consequently, the two Tevatron experiments, D0 and CDF, have served as prominent arenas for studying hadronic jets.

In this Letter, we report a new measurement of the pseudorapidity (η) and transverse-energy (E_T) dependence of the inclusive jet production cross section [6], which examines the short-range behavior of QCD, the structure of the proton in terms of PDFs, and possible substructure of quarks and gluons. We present the differential cross section $d^2\sigma/(dE_T d\eta)$ as a function of jet E_T in five intervals of η, up to $|\eta| = 3$, where the pseudorapidity is defined as $\eta = \ln[\cot(\theta/2)]$, with θ being the polar angle. The present measurement is based on 95 pb^{-1} of data collected with the D0 detector [7] during 1994–1995, and significantly extends previous measurements [8], as indicated by the kinematic reach shown in Fig. 1.

The primary tool used for jet detection is the compensating, finely segmented, liquid-argon/uranium calorimeter, which provides nearly full solid-angle coverage ($|\eta| < 4.1$). Jets are defined and reconstructed off-line using an iterative fixed-cone algorithm with a cone radius of $\mathcal{R} = 0.7$ in the η-φ space, where φ is the azimuth. The missing transverse energy ($\not{E}_T$) is calculated from a vector sum of the individual E_T values in all the cells of the calorimeter. Calorimeter cells can occasionally provide spurious noise signals; to diminish their effect on jets, such cells are identified and suppressed using specific on-line and off-line algorithms.

During data taking, events were selected with a multi-stage trigger system. The first stage signaled an inelastic $p\bar{p}$ collision. In the next stage, the trigger required a jet in a calorimeter region of $\Delta\eta \times \Delta\varphi = 0.8 \times 1.6$, with E_T above a preset threshold. In the last trigger stage, selected events were digitized and sent to an array of processors. Jet candidates were reconstructed using a cone algorithm, and the entire event was recorded if any jet E_T exceeded a specified threshold. The four software filters used in this analysis had E_T thresholds of 30, 50, 85, and 115 GeV, and accumulated integrated luminosities of 0.364, 4.84, 56.5, and 94.9 pb^{-1}, respectively [9]. To present the full range of the data, the cross sections obtained from the four jet filters are combined in contiguous regions of E_T in such a way that the more restrictive trigger is adopted as soon as it is more than 99% efficient.

The position of the primary interaction vertex is reconstructed using data from the central tracking system. The two vertices with the largest number of associated tracks are retained for further analysis. At high instantaneous luminosities, multiple interactions are common, and to correct for inefficiency of the tracking system in identifying the primary vertex, we use the global event quantity $S_T = |\sum \vec{E}_T^{\text{jet}}|$. The vertex with the smaller value of S_T is defined
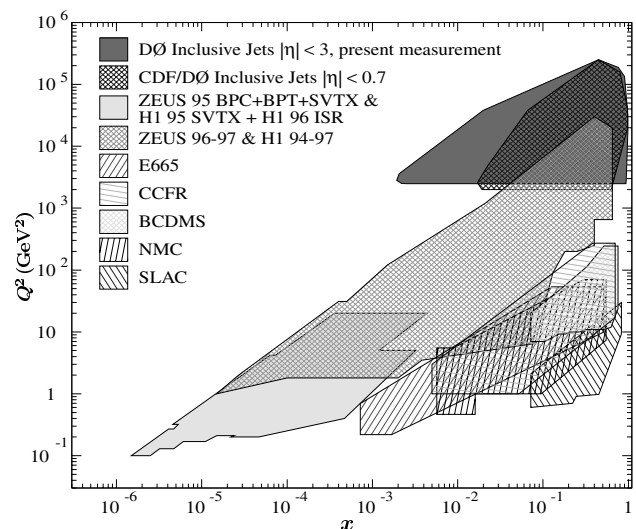

FIG. 1. The kinematic reach of this measurement along with that of other collider and fixed-target experiments in the plane of the parton momentum fraction x and the square of the momentum transfer Q^2.

as the correct event vertex, and all kinematic variables are calculated with respect to it. The dependence of jet E_T on luminosity was studied, and found to be negligible. At high pseudorapidities, the jet reconstruction algorithm introduces a bias towards $\eta = 0$. Furthermore, the Snowmass jet reconstruction algorithm [10] used in the theoretical predictions has a different definition for jet angles than that used in the standard D0 off-line algorithm. Jet η values are corrected for this difference, which also removes any instrumental bias in reconstruction of jet polar angles [6].

Backgrounds introduced by electrons, photons, detector noise, accelerator losses, or cosmic rays are removed using quality criteria developed for jets with $|\eta| \leq 3$. To preserve the pseudoprojective nature of the D0 calorimeters, the longitudinal (z) position of the interaction vertex is required to be within 50 cm of the detector center; this requirement is $(88.7 \pm 0.1)\%$ efficient. A cutoff on $\not{E}_T$ removes background from cosmic ray showers and misvertexed events. $\not{E}_T$ must be smaller than the lesser of 30 GeV or $0.3E_T$ of the leading jet if the leading jet is central ($|\eta| < 0.7$), or less than $0.7E_T$ otherwise. This criterion is nearly 100% efficient. Jet quality is based on the pattern of energy deposition in the calorimeter. The combined efficiency for jet quality ranges from about 99.5% at lowest E_T and $|\eta|$ to approximately 98% at highest E_T and $|\eta|$.

The jet energy calibration, applied on a jet-by-jet basis, corrects (on average) the reconstructed E_T for variation in the hadronic response of the calorimeter, for the energy associated with underlying spectator interactions, for multiple $p\bar{p}$ interactions in the same crossing, noise originating from uranium decay, the fraction of any particle's energy that showers outside of the reconstruction cone, and for detector nonuniformities. A complete discussion of the jet energy calibration can be found in Ref. [11]. An independent test of the jet energy scale, based on the balance in transverse energy in photon-jet and jet-jet data, confirms the validity of the D0 jet-calibration procedure up to $|\eta| = 3$ [6].

In each bin of η-E_T, the average differential cross section, $d^2\sigma/(dE_T d\eta)$, is calculated as $N/(\Delta\eta\Delta E_T \epsilon \times \int \mathcal{L}\, dt)$, where $\Delta\eta\Delta E_T$ is the η-E_T bin size, N is the number of jets observed in a bin, ϵ is the total overall efficiency for jet and event selection, and $\int \mathcal{L}\, dt$ represents the integrated luminosity of the data sample. Statistical uncertainties in the values of the cross sections are defined by 1 standard deviation Poisson fluctuations in the associated N.

Energy resolution of the D0 calorimeters distorts the jet cross section in E_T. Although the resolution is essentially Gaussian, the jet cross section is shifted to larger E_T due to the steeply falling dependence of jet production on E_T. This effect is removed from the data through an unfolding procedure. We measure the fractional jet energy resolutions based on the "same side" ($\eta_1 \cdot \eta_2 > 0$) subset of dijet events in the data sample. Using the imbalance in the E_T of the two leading jets, in each interval of $|\eta|$, we pa-

rametrize the fractional jet energy resolution as a function of jet E_T, following the standard description of single-particle energy resolution, based on the noise, sampling, and constant terms. To determine the amount of distortion in the cross section in each of the five $|\eta|$ intervals, we take an ansatz function of the form $e^\alpha E_T^\beta (1 + \gamma 2E_T/\sqrt{s})^\delta$, numerically smear it according to the parametrized resolution in each E_T bin, and fit this smeared hypothesis to the observed cross sections to extract the five sets of four free parameters, α, β, γ, and δ. The bin-by-bin ratio of the original over the smeared ansatz for each range of $|\eta|$ gives the unfolding correction with which we rescale the observed cross section to remove the distortion from jet energy resolution [6].

The jet angular resolution is very good at all η, and its effect on the cross section is negligible, but it is possible to distort the jet polar angle through a mismeasurement of the z position of the vertex. However, a Monte Carlo study demonstrates that such effects are negligible because distortions in jet E_T are nearly fully compensated by bin-to-bin migrations in $|\eta|$ from the smearing of the z coordinate of the vertex [6].

The final measurements in each of the five $|\eta|$ regions, along with statistical uncertainties, are presented in Fig. 2 (tables of the measured cross sections can be found in Refs. [6,12]). The measurement spans about 7 orders of magnitude and extends to the highest jet energies ever reached. Figure 2 also shows $\mathcal{O}(\alpha_s^3)$ theoretical predictions from JETRAD [3] with renormalization and factorization scales set to half of the E_T of the leading jet and using the CTEQ4M PDF.

Figures 3 and 4 provide more detailed comparisons to predictions on a linear scale for several PDFs (for other
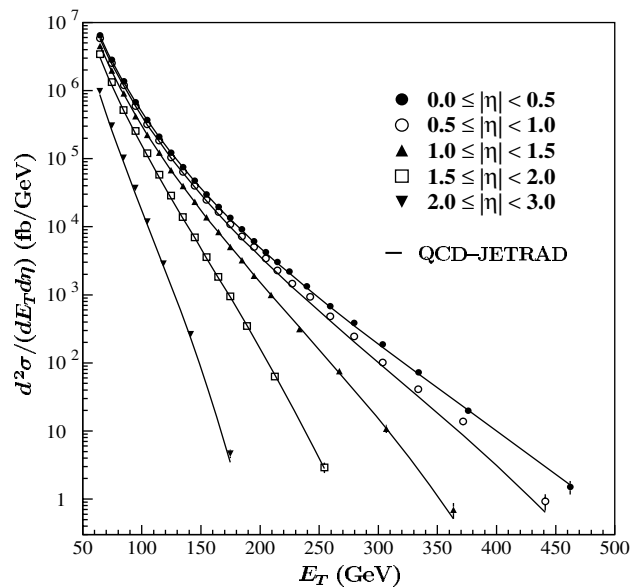

FIG. 2.   The single inclusive jet production cross section as a function of jet E_T, in five pseudorapidity intervals, showing only statistical uncertainties, along with theoretical predictions.
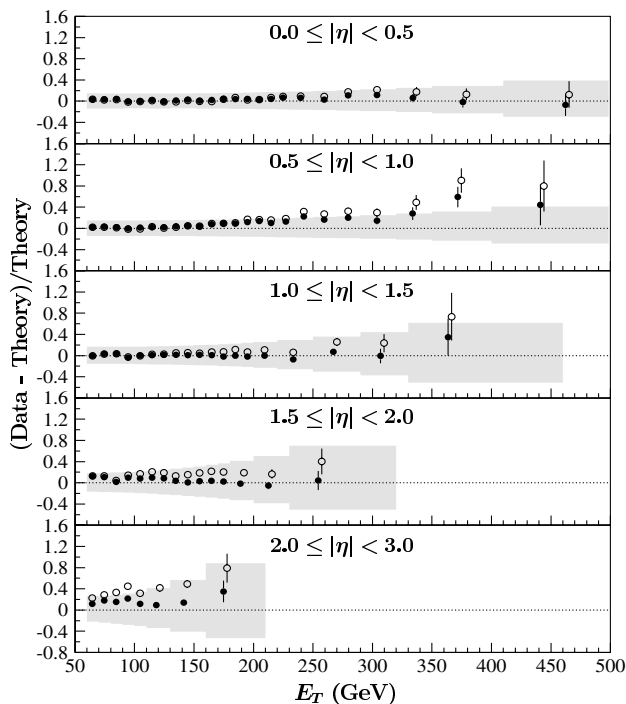
FIG. 3. Comparisons between the D0 single inclusive jet cross sections and the $\mathcal{O}(\alpha_s^3)$ QCD predictions calculated by JETRAD with the CTEQ4HJ ($\bullet$) and CTEQ4M ($\circ$) PDFs. The highest E_T points are offset slightly for CTEQ4M.
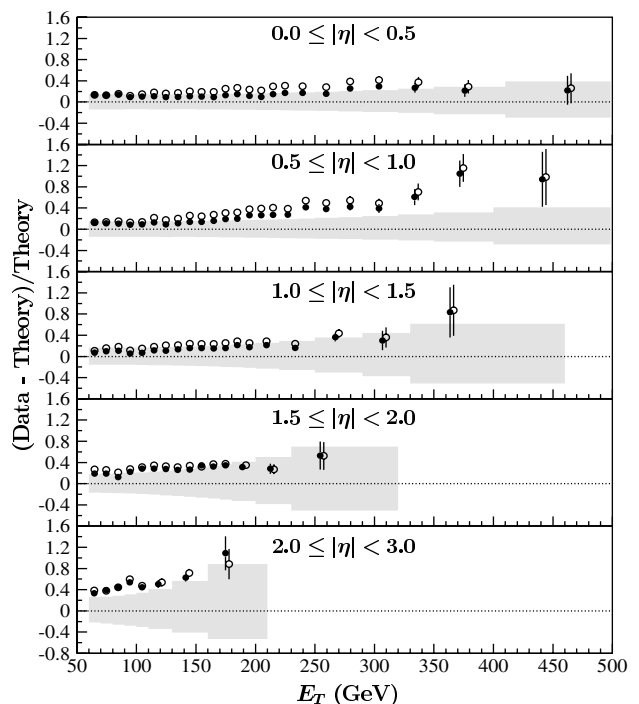
FIG. 4. Comparisons between the D0 single inclusive jet cross sections and the $\mathcal{O}(\alpha_s^3)$ QCD predictions calculated by JETRAD with the MRSTg↑ ($\bullet$) and MRST ($\circ$) PDFs. The highest E_T points are offset slightly for MRST.

PDFs, see Ref. [6]). The error bars are statistical, while the shaded bands indicate 1 standard deviation systematic uncertainties. Because the theoretical uncertainties due to variations in input parameters are comparable to the systematic uncertainties [13], these qualitative comparisons indicate that the predictions are in reasonable agreement with the data for all $|\eta|$ intervals.

To quantify the comparisons, we employ a specially derived and previously studied χ^2 statistic of the form [6,9] $\chi^2 = \sum_{i,j}(D_i - T_i)[(T_i/D_i)C_{ij}(T_j/D_j)]^{-1}(D_j - T_j)$, where $(D_i - T_i)$ is the deviation of the measured cross section (D_i) from the prediction (T_i) in the ith bin, C_{ij} is the full covariance matrix of the measurement [12], defined as $\sum_{\alpha} \rho_{ij}^{\alpha} \sigma_i^{\alpha} \sigma_j^{\alpha}$, where the sum runs over all sources of uncertainties, ρ_{ij} is the correlation coefficient between the ith and jth bins, and σ_i is the uncertainty in the ith bin. The T/D factors are introduced to reduce the bias towards lower values of χ^2 originating from highly correlated systematic uncertainties present in C_{ij} [9]. There are 90 η-E_T bins in this measurement.

While the statistical uncertainties are not correlated in E_T or η, the systematic uncertainties are fully correlated in both variables except for (i) efficiencies for data selection, which are uncorrelated in η, (ii) parametrizations of jet energy resolutions and fits to the unfolding ansatz, which are uncorrelated in η, (iii) the hadronic response, which is partially correlated in E_T and η, with the correlation matrix in terms of average bin energies given in Ref. [11]. Uncertainties in the showering correction arise dominantly from

the lack of full agreement of the lateral shower profiles observed in the data and in the Monte Carlo. The residual discrepancy is similar for all E_T and η regions. Consequently, the correlations of the showering correction are large in E_T [14] as well as in η. Uncertainties due to jet energy calibration are the dominant source of error in the cross section and range from about 12%–20% at lowest E_T to about 35%–80% at highest E_T, getting larger with η for a fixed E_T. They are driven by the uncertainties due to the hadronic response parametrization at high E_T and due to the showering correction at high E_T and, notably, at high η. The second largest source of uncertainty is the jet energy resolution parametrization and the unfolding procedure which typically gets worse at low and at high E_T and ranges from about 3%–5% at lowest E_T to about 10%–20% at highest E_T. These are followed by the uncertainties due to integrated luminosity which are approximately 6% (8%) for the data collected with the jet filters with two highest (lowest) E_T thresholds, and by the uncertainties due to data selection which are on the order of 1% throughout the dynamic range of the measurement [6].

For all PDFs we have considered, Table I lists the χ^2, χ^2/d.o.f., and the corresponding probabilities for 90 degrees of freedom (d.o.f.). We have verified that the variations of correlation coefficients within the range of their uncertainties give a similar ordering of the χ^2, hence a similar relative preference of PDFs. The absolute values of χ^2 and associated probabilities vary somewhat with variations in the correlations in E_T and, to a much lesser extent,

TABLE I. The χ^2, χ^2/d.o.f., and the corresponding probabilities for 90 degrees of freedom for various PDFs studied.

PDF	χ^2	χ^2/d.o.f.	Probability
CTEQ3M	121.56	1.35	0.01
CTEQ4M	92.46	1.03	0.41
CTEQ4HJ	59.38	0.66	0.99
MRST	113.78	1.26	0.05
MRSTg↓	155.52	1.73	<0.01
MRSTg↑	85.09	0.95	0.63

with variations of correlations in η. The theoretical predictions are in good quantitative agreement with the experimental results. The data indicate a preference for the CTEQ4HJ, MRSTg↑, and CTEQ4M PDFs. The CTEQ4HJ PDF has enhanced gluon content at large x, favored by previous measurements of inclusive jet cross sections at small η [14,15], relative to the CTEQ4M PDF. The MRSTg↑ PDF includes no intrinsic parton transverse momentum and therefore has effectively increased gluon distributions at all x relative to the MRST PDF.

In conclusion, we have reported a new measurement of the pseudorapidity and transverse-energy dependence of the inclusive jet cross section in proton-antiproton collisions at $\sqrt{s} = 1.8$ TeV. Our results extend significantly the kinematic reach of previous studies, are consistent with QCD calculations over the large dynamic range accessible to D0 ($|\eta| < 3$), and indicate a preference for certain PDFs. Once incorporated into revised modern PDFs, these measurements will greatly improve our understanding of the structure of the proton at large x and Q^2.

[1] S. D. Ellis, Z. Kunszt, and D. E. Soper, Phys. Rev. Lett. **64**, 2121 (1990).

[2] F. Aversa *et al.,* Phys. Rev. Lett. **65**, 401 (1990).

[3] W. T. Giele, E. W. N. Glover, and D. A. Kosower, Phys. Rev. Lett. **73**, 2019 (1994).

[4] H. L. Lai *et al.,* Phys. Rev. D **51**, 4763 (1995); **55**, 1280 (1997).

[5] A. D. Martin *et al.,* Eur. Phys. J. C **4**, 463 (1998).

[6] L. Babukhadia, Ph.D. thesis, University of Arizona, 1999 (unpublished), http://fnalpubs.fnal.gov/techpubs/theses.html.

[7] D0 Collaboration, S. Abachi *et al.,* Nucl. Instrum. Methods Phys. Res., Sect. A **338**, 185 (1994).

[8] Particle Data Group, D. E. Groom *et al.,* Eur. Phys. J. C **15**, 1 (2000).

[9] D0 Collaboration, B. Abbott *et al.,* Report No. Fermilab-Pub-00/216-E, 2000.

[10] J. Huth *et al.,* in *Proceedings of Research Directions for the Decade, Snowmass 1990,* edited by E. L. Berger (World Scientific, Singapore, 1992).

[11] D0 Collaboration, B. Abbott *et al.,* Nucl. Instrum. Methods Phys. Res., Sect. A **424**, 352 (1999); A. Goussiou, Report No. Fermilab-Pub-99/264-E, 1999.

[12] See AIP Document No. EPAPS: E-PRLTAO-86-054109 for cross section tables and the covariance matrix of the measurement. This document may be retrieved via the EPAPS homepage (http://www.aip.org/pubservs/epaps.html) or from ftp.aip.org in the directory /epaps/. See the EPAPS homepage for more information.

[13] D0 Collaboration, B. Abbott *et al.,* Eur. Phys. J. C **5**, 687 (1998).

[14] D0 Collaboration, B. Abbott *et al.,* Phys. Rev. Lett. **82**, 2451 (1999).

[15] CDF Collaboration, F. Abe *et al.,* Phys. Rev. Lett. **77**, 438 (1996).